

# Polycrystalline Diamonds from Kimberlites: Snapshots of Rapid and Episodic Diamond Formation in the Lithospheric Mantle

**Dorrit E. Jacob\***

*Research School of Earth Sciences  
The Australian National University  
Canberra, Australia  
dorrit.jacob@anu.edu.au*

**Sami Mikhail\***

*The School of Earth and Environmental Sciences  
University of St. Andrews  
United Kingdom  
sm342@st-andrews.ac.uk*

*\*both authors contributed equally to this chapter*

## INTRODUCTION

Monocrystalline diamonds are the most valuable diamond type, economically. However, there are other varieties of diamond forged in Earth's lithospheric mantle, which, while not economically profitable, are of considerable value to the geosciences. Most prominent amongst these are fibrous diamonds (Weiss et al. 2022, this volume) and polycrystalline diamond aggregates (PDAs). Polycrystalline diamond aggregates are rocks in which the dominant mineral phase is diamond (Fig. 1), whereas fibrous diamonds are cuboid samples, sometimes with monocrystalline diamond cores and cloudy overgrowths ('coats'), or octahedral diamonds with fibrous cores (Weiss et al. 2022, this volume). The fibrous growth sectors are highly imperfect single crystals hosting millions of fluid and solid micro-inclusions (Navon et al. 1988). Polycrystalline diamond aggregates (PDAs) from kimberlites are the least well-studied of the diamond family. This chapter aims to showcase what we know of PDA-formation in the context of monocrystalline diamond formation, the origin of carbon enrichment in the cratonic lithosphere, and the identify the relationship(s) between polycrystalline diamond formation and plate tectonics.

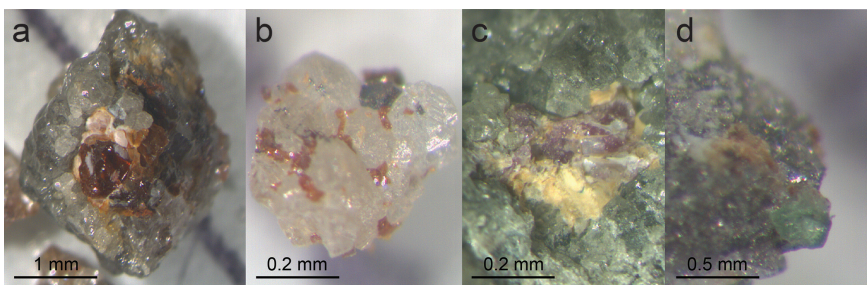


**Figure 1.** Images of silicate-bearing polycrystalline diamond aggregates from Orapa (a–d, from Mikhail et al. 2019b).

## NOMENCLATURE

Nothing better serves to illuminate the blurred line between academia and industry in diamond science than the diversity of, and etymology behind, the nomenclature applied to polycrystalline diamond. The most commonly used names are framesite, stewartite, diamondite, boart, and carbonado (Table 1). The names used to sub-divide the group originate from the lexica of both industry and academia and are based on appearance (e.g., grain size), application, value, and in some cases, physical properties. For instance, if a polycrystalline diamond aggregate contains unidentified or identified magnetic phases (presumably magnetite) then it can be termed stewartite, but if the sample is non-magnetic then the name framesite can be applied (Heaney et al. 2005). These names derive from two persons named Stewart and Frames, former mine managers at the Cullinan Mine (Andy Moore, pers. comm. 2021). Both, stewartite and framesite can also be referred to as boart, which means the sample is not a single crystal and is not of gem quality, but that the sample is suitable for use as an abrasive. The etymology of the word diamondite follows a standard geological/petrographic classification scheme where rocks can be named according to their dominant mineral phase. For example, if a rock is dominantly comprised of clino- and/or ortho-pyroxene then it can be called a pyroxenite, and so the argument was put forward that mantle xenoliths dominated by diamond should be referred to as diamondite (Kurat and Dobosi 2000). Stewartite is the least commonly used name, either because most samples are non-magnetic or because most people do not check whether or not a framesite/diamondite is magnetic.

The carbonados are considered by most researchers to be a diamond sub-group of their own. Carbonados are dark-colored, equidimensional, microporphyritic and often have a glassy diamond patina that can show slickensides (Haggerty 2017). In short, carbonados do not look like the polycrystalline diamond aggregates found in kimberlites. Like PDAs associated with kimberlites, carbonados are porous, with about 10–15% pore space, but the pores are rounded rather than polygonal (Haggerty 2017). The primary host rock for carbonados is unknown. They are found exclusively in an alluvial setting in Mid-Proterozoic (1–1.5 Ga) metaconglomerates overlying the São Francisco and Congo-Kasai cratons in Brazil and in Mesozoic sandstones in the Central African Republic (Fettke and Sturges 1933; Leonardos 1937; Trueb and De Wys 1969; Haggerty 1999). The two localities are paleo-geographically connected and once formed part of the supercontinent Rodinia (De Waele et al. 2008). The intergrowths and inclusions described from carbonados feature phases not usually associated with diamond from the Earth's mantle. They comprise phases associated with crustal and sedimentary rocks, such as florencite-goyazite-gorceixite, xenotime, kaolinite, quartz, orthoclase, zircon, and also a suite of very reducing phases, such as SiC, TiN, and Fe, Fe–Ni, W–Fe–Cr–V, Ni–Cr, Si, Sn metallic

**Table 1.** Polycrystalline diamond aggregate terminology and characteristics.

Name	Defining characteristics
Framesite	Polycrystalline and non-magnetic
Stewartite	Polycrystalline and magnetic
Boart	Morphology is not economically viable and comprises >1 diamond crystal
Diamondite	Any polycrystalline aggregate where diamond is the most abundant mineral phase
Carbonado	Black, polycrystalline, and only found in the Mid-Proterozoic (1–1.5 Ga) metaconglomerate overlying the São Francisco and Congo-Kasai cratons

and alloyed phases (Heaney et al. 2005; Haggerty 2014). The mixture of uncommon syngenetic and epigenetic inclusions, including crustal inclusions, have been posing a challenge to develop models explaining their genesis which encompass a wide range of scenarios, including extraterrestrial origins (Heaney et al. 2005; Haggerty 2014). As carbonados are geologically much less constrained than polycrystalline diamond aggregates from kimberlites there is a risk that the new findings for the kimberlitic PDAs do not apply to carbonado. Consequently, a summary of the carbonado literature in this chapter would contribute little that has not been said before. For details on carbonado, we direct the reader to the extensive reviews existing in the literature for carbonados, such as Haggerty (2014, 2017) and Heaney et al. (2005).

Herein, we use the term “polycrystalline diamond aggregate” (PDA) to group all polycrystalline samples (Fig. 1). This review is concerned with the origin and geological significance of PDAs from kimberlites which host silicates and oxides. This is because their direct association with kimberlites and their intergrowths/inclusions provide *bona fide* geological context, without which all inferences are devoid of any meaningful relation with geological processes, or events.

## POLYCRYSTALLINE DIAMOND AGGREGATES FROM KIMBERLITES

To our knowledge, polycrystalline diamond aggregates (Fig. 1) have, thus far, only been reported in the peer-reviewed literature from Group I kimberlites. PDAs amount to as much as 20% of the diamond production in Southern African and Yakutian kimberlites, including Orapa, Venetia, Cullinan (Premier), Jwaneng, Mirny, Aikhal, Yubileinaya and Sytykanskaya (Orlov 1977; Kaminsky et al. 1981; Gurney and Boyd 1982; McCandless et al. 1989; Smelova 1994; Kirkley et al. 1995; Jacob et al. 2000; Sobolev et al. 2016). PDAs can be up to several centimetres in size (several hundred carats) and comprise randomly oriented diamonds of variable size from ca. 5  $\mu\text{m}$  to 5,000  $\mu\text{m}$  (Sobolev 1977; Rubanova et al. 2012) intergrown with silicates, oxides and other phases (Jacob et al. 2011). An important and notable difference to inclusions in monocrystalline diamonds is that non-diamond phases in PDAs are *intergrown* with the diamond grains, confirming a petrogenetic relationship, rather than representing material trapped during diamond formation or random epigenetic phases. Individual diamonds in PDAs are also found included in the non-diamond phases, indicating the syngenetic formation of diamond, silicate, oxides, carbide, and fluid components (Kurat and Dobosi 2000; Jacob et al. 2004; Mikhail et al. 2019b).

The high porosity of some PDAs (up to 30%; Heaney et al. 2005; Jacob et al. 2011), the release of detectable  $^3\text{He}$  when crushed under vacuum (Gautheron et al. 2005; Mikhail et al. 2019a), and the presence of trace amounts of hydrogen (e.g.,  $38 \pm 5$  ppm; Fourel et al. 2017) indicate the presence of fluids trapped during formation. In some cases, it appears that these intergrowths are not shielded from their surroundings and can thus be subject to metasomatic alteration. For example, a micro-computed tomography ( $\mu\text{CT}$ ) study of a PDA sample from Orapa, Botswana (Jacob et al. 2011) presents spectacular hematite alteration rims around magnetite (Fig. 2), illustrating epigenetic metasomatic changes facilitated by the high porosity and permeability in some PDAs.

This chapter summarizes data on the diamond and non-diamond components in kimberlite-related PDAs. This information is synergized into a narrative of what we know and what we will still need to know as informed by these data. We show how the geochemical and petrological insights distinguish PDAs from the monocrystalline diamond types (gem and fibrous types) and explain what they reveal about our collective understanding of mantle metasomatism, tectonic volatile fluxing, and the deep carbon cycle.

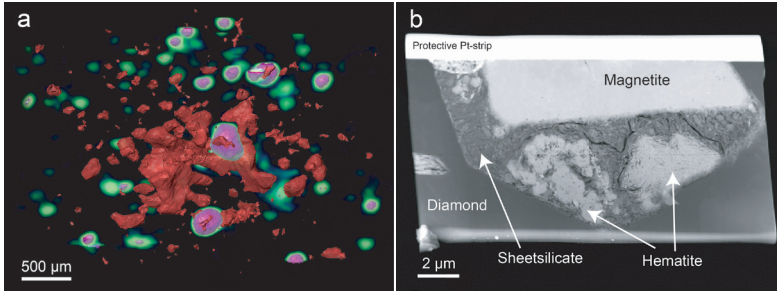


**Figure 2.** (a)  $\mu$ CT region of interest showing pore space (red) and magnetite grains (purple) covered by a replacement envelope (green) of a mixture of hematite and a sheet silicate. Diamonds are rendered transparent in this view. (b) TEM HAADF image of a FIB foil cut from a diamond grain showing a replacement rim around magnetite consisting of a mixture of hematite and a sheet silicate.

## INSIGHTS FROM DIAMOND GEOCHEMISTRY

Polycrystalline diamond growth is the result of heterogeneous nucleation and rapid crystal growth driven mainly by carbon supersaturation (Sunagawa 2005). Hence, while monocrystalline diamonds can show extended histories of slow growth (Howell et al. 2012b; Timmerman et al. 2019a), PDA formation appears to be rapid (Orlov 1977). Therefore, because of their rapid formation, both fibrous diamonds and polycrystalline diamond aggregates provide important and complementary perspectives on diamond formation processes compared to the time-integrated story recorded by some monocrystalline diamonds.

### Source(s) of diamond-forming metasomatic fluids

The origin of PDA-forming fluids has been evaluated using the  $\delta^{13}\text{C}$  and  $\delta^{15}\text{N}$  values for the diamond component of PDAs (Shelkov et al. 1997; Jacob et al. 2000; Maruoka et al. 2004; Mikhail et al. 2013, 2014c), and using helium isotope constraints from micro- to nano-inclusions in the rocks (Burgess et al. 1998; Gautheron et al. 2005; Mikhail et al. 2019a).

The stable isotope ratios of carbon and nitrogen for crustal and mantle derived material show distinctions between their average values (Hoefs 2009 and references therein) (Fig. 3). Hence, for diamonds, these stable isotope systems can be useful indicators for their sources and elucidate crust–mantle interaction (Stachel et al. 2022, this volume). This picture is complicated due to significant stable isotope fractionation effects, which can occur at high temperatures and pressures and in associated closed and open system diamond formation processes (Stachel et al. 2022, this volume). Owing to the similarity of the mass difference between the heavy and light isotopes for carbon and nitrogen, the equilibrium stable isotope fractionation factors for carbon and for nitrogen are similar in magnitude at mantle temperatures, and these are usually within 1–2‰ depending on the species involved (Richet et al. 1977; Deines 1980; Polyakov and Kharlashina 1995; Reutsky et al. 2008, 2015; Petts et al. 2016). However, the specific fractionation reactions in the Earth's mantle seem to play a bigger role for carbon (e.g., decarbonation) than for nitrogen (Cartigny et al. 2014; Petts et al. 2016). Progressive fractionation of an evolving fluid in a closed system (i.e., Rayleigh fractionation) has been suggested to explain monocrystalline diamonds that display continuous, coupled changes in carbon and nitrogen isotopic values (Petts et al. 2015). On the other hand, open system mixing of fluids (e.g., Petts et al. 2015) or separate fluid pulses with different isotopic compositions (e.g., Wiggers de Vries et al. 2013; Smit et al. 2016) have been suggested to explain the observed variability in the carbon and nitrogen isotope values of some other diamonds, including PDAs (Jacob et al. 2017 and Fig. 4). Thus, nitrogen concentrations of diamonds and their corresponding nitrogen isotope values ( $\delta^{15}\text{N}$ ) complement the  $\delta^{13}\text{C}$  values to trace the source of diamond-forming fluids in the deep Earth (Javoy et al. 1986; Boyd and Pillinger 1994; Cartigny et al. 1998a).

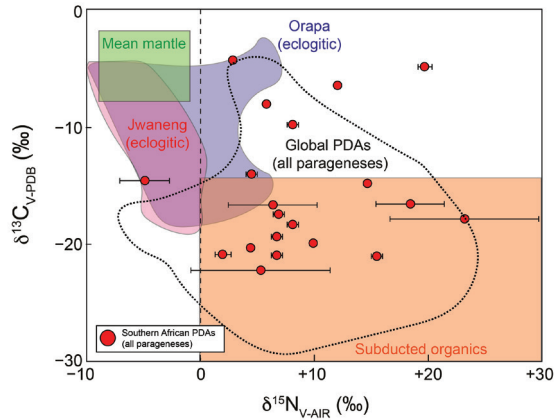


**Figure 3.** Plot of  $\delta^{13}\text{C}$  vs  $\delta^{15}\text{N}$  values for select diamond types. Shown here is the mean mantle C–N stable isotope field, within which most fibrous diamonds plot (compiled by Cartigny et al. 2014). Also shown are the fields for eclogitic monocrystalline diamonds from Jwaneng and Orapa (Cartigny et al. 1998b, 1999). The PDA data are from Gautheron et al. (2005), Maruoka et al. (2004), and Mikhail et al. (2013, 2014a, 2019b). The data for the  $\delta^{13}\text{C}$  and  $\delta^{15}\text{N}$  values for subducted organics are from Halama et al. (2010, 2014) Busigny et al. (2019), and the compilation in Cartigny et al. (2014).

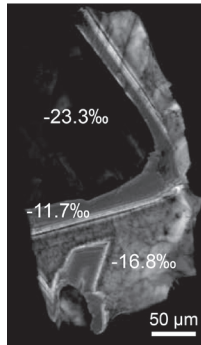


**Figure 4.** Cathodoluminescence image of a diamond fragment from a websteritic PDA from Venetia showing different growth zones with variable  $\delta^{13}\text{C}$  values, indicating different growth pulses.

In general, PDA diamond geochemistry is characterized by  $^{13}\text{C}$ -depletion and  $^{15}\text{N}$ -enrichment, higher than average nitrogen abundances, a lower than average occurrence of nitrogen-free samples, and a range of nitrogen aggregation states (Mikhail et al. 2019b and references therein). The carbon isotope values for PDAs show a large range from  $\delta^{13}\text{C} = -1\text{‰}$  to  $-30\text{‰}$  (Fig. 3) with modes at  $-5\text{‰}$  and  $-18\text{‰}$  (Deines 1980; Maruoka et al. 2004; Mikhail et al. 2013, 2019b; Jacob et al. 2014; Sobolev et al. 2016). However, when plotting only those data where combined C–N isotope systematics for garnet-bearing PDA samples are considered (to enable meaningful comparisons between the different isotopic and paragenetic systems), the mode at  $-5\text{‰}$  is not present. It is noteworthy that, alongside peridotitic and websteritic PDAs only a small subset of eclogitic and websteritic monocrystalline diamonds show  $^{13}\text{C}$ -depletion with mean values positioned lower than the  $-20\text{‰}$  (e.g., eclogitic samples from Dachine (French Guiana; Smith et al. 2016) and Jericho (Northern Canada; De Stefano et al. 2009). However, what distinguishes the PDAs from monocrystalline diamonds is the fact that all parageneses (eclogitic, websteritic, and peridotitic) are found to show  $^{13}\text{C}$ -depletion (Maruoka et al. 2004; Mikhail et al. 2014a, 2019b), with a mode at  $-18\text{‰}$ , while peridotitic monocrystalline diamonds plot with the mode at  $-5\text{‰}$  (Table 2).

**Table 2.** Averages for samples where combined N and C data are available (no data considered when only one of the isotope systems is reported). Note the large standard deviations for the mean nitrogen concentrations for PDAs reflecting the large ranges of concentrations and the absence of a significant mean nitrogen abundance for PDAs. Data sources: monocrystalline diamond (Cartigny et al. 1997, 1998a, b, 1999, 2004, 2009; Palot et al. 2009; Thomassot et al. 2009; Cartigny 2010; Palot et al. 2012; Mikhail et al. 2014b; Smith et al. 2016), fibrous diamond (Javoy et al. 1986; Boyd et al. 1987, 1992; Klein-BenDavid et al. 2010), and PDAs (Javoy et al. 1986; Boyd et al. 1987, 1992; Shelkov 1997; Klein-BenDavid et al. 2010).

Diamond Type	<i>n</i>	$\delta^{13}\text{C}$ (‰)	StDev	$\delta^{15}\text{N}$ (‰)	StDev	N at.ppm	StDev
Monocrystalline (Peridotitic)	189	-4.6	1.9	-4.9	7.0	396	350
Monocrystalline (Eclogitic)	204	-9.5	8.2	-2.9	5.7	649	483
Fibrous	109	-6.5	3.1	-1.6	4.4	922	360
PDA	62	-18.1	5.4	+8.4	6.7	469	715

The  $\delta^{15}\text{N}$  values range from  $-6.1\text{‰}$  to  $+22.6\text{‰}$  (Gautheron et al. 2005; Mikhail et al. 2014c; Jacob et al. 2017) with an average of  $+8.4\text{‰}$  (Table 2)—an average value that is significantly more  $^{15}\text{N}$ -enriched than for all other diamond types (Table 2). The  $^{15}\text{N}$ -enrichment in PDAs is important because the interior and exterior of Earth show a pronounced and statistically significant isotopic disequilibrium for nitrogen, where the upper mantle is  $^{15}\text{N}$ -depleted and the crustal reservoirs are  $^{15}\text{N}$ -enriched (Boyd and Pillinger 1994). Thus, the  $^{15}\text{N}$ -enriched nature of PDAs supports involvement of crustal material in their formation. In addition, oxygen isotopic values for garnets in PDAs from Venetia (Jacob et al. 2000) and Orapa (Mikhail et al. 2019b) show  $\delta^{18}\text{O}$  values from  $+5.96$  to  $+8.09\text{‰}$ , which are higher than  $\delta^{18}\text{O}$  values for the ambient mantle ( $\delta^{18}\text{O} = 5.5\text{‰}$ ; Matthey and MacPherson 1993). The origin of  $^{18}\text{O}$ -enriched or depleted oxygen in mantle samples is considered to be *bona fide* evidence for material altered in a thermal environment of too low energy to be assignable to the deep Earth, this is based on evidence that equilibrium stable isotope fractionation for  $^{18}\text{O}/^{16}\text{O}$  at temperatures  $> 800\text{ °C}$  and at high pressures are negligible and cannot explain a shift of  $\delta^{18}\text{O}$  value  $> \pm 1\text{‰}$  (Chacko et al. 2001).

The nitrogen concentrations in PDAs cover a large and unevenly distributed range from 4 to 3635 at.ppm N with an average nitrogen abundance of  $496 \pm 715$  ppm (Table 2). These nitrogen concentration data are not resolvable from monocrystalline diamonds or fibrous diamond samples, but the latter show higher average nitrogen abundances of around  $922 \pm 360$  ppm. The different average nitrogen concentrations unfortunately do not carry much significance due to the overlap of the datasets and considering the spread of data. In general, the spread of nitrogen concentrations in PDAs are not dissimilar from every other diamond type, where monocrystalline samples show lower average nitrogen abundances with  $396 \pm 350$  and  $649 \pm 483$  ppm for peridotitic and eclogitic monocrystalline samples, respectively (Cartigny 2005). These poorly defined averages for the nitrogen concentrations in mantle diamonds are sometimes used to argue for kinetic uptake of nitrogen in diamond during growth, where the slow diffusion of nitrogen in diamond (Koga et al. 2003) prohibits re-equilibration after formation (see Mikhail and Howell 2016, for a discussion). Compared to the concentrations of nitrogen, the stable isotope data are significantly distinct in their distribution and significance. Collectively, the role for a subducted crustal organic component for the significant  $^{13}\text{C}$ -depletion is supported by the high nitrogen concentrations and very positive nitrogen isotope values for PDAs (Shelkov et al. 1997; Gautheron et al. 2005; Jacob et al. 2014, 2017; Mikhail et al. 2014c, 2019a) because the combined  $\delta^{13}\text{C}$  vs  $\delta^{15}\text{N}$  vs N ppm data are typical for material from Earth's surface (Boyd and Pillinger 1994).

When crushed under vacuum, PDAs release gas (Gautheron et al. 2005; Mikhail et al. 2019a), and this requires the presence of fluid micro-inclusions to explain the release of detectable  $^3\text{He}$  after crushing (Gautheron et al. 2005; Mikhail et al. 2019a). Therefore, to shed more light on the origin of diamond-forming fluids one can apply noble gas isotope data to complement and test hypotheses developed using C–N stable isotope data (e.g.,  $^3\text{He}/^4\text{He}$ ). This is useful because, while C and N isotope systems are powerful tracers of subducted material,  $^3\text{He}$  is an equally powerful tracer for an otherwise hidden mantle signature within crustal-source dominated  $^{13}\text{C}$ -depleted and  $^{15}\text{N}$ -enriched systems. This is because  $^3\text{He}$  is a primordial isotope and one of the most incompatible elements in silicate systems (Brooker et al. 2003; Jackson et al. 2013). Therefore,  $^3\text{He}$  is not transferred into the solid Earth after degassing (instead, it is so light that it is lost to space). However, an unavoidable issue is  $^4\text{He}$  ingrowth due to radioactive alpha decay. The degree of nitrogen aggregation in PDAs, fibrous and monocrystalline diamonds is consistent with millions to billions of years of mantle residence (Mikhail et al. 2019a and references therein) permitting  $^4\text{He}$  growth due to alpha decay of U and Th in the sample, which decreases the  $^3\text{He}/^4\text{He}$  ratios over time (Timmerman et al. 2019a, b). This results in a relationship between  $^3\text{He}/^4\text{He}$  and  $^3\text{He}$  concentration shown in Figure 5, reflecting radiogenic  $^4\text{He}$  production since the fluids were trapped in diamond (see caption to Fig. 5).

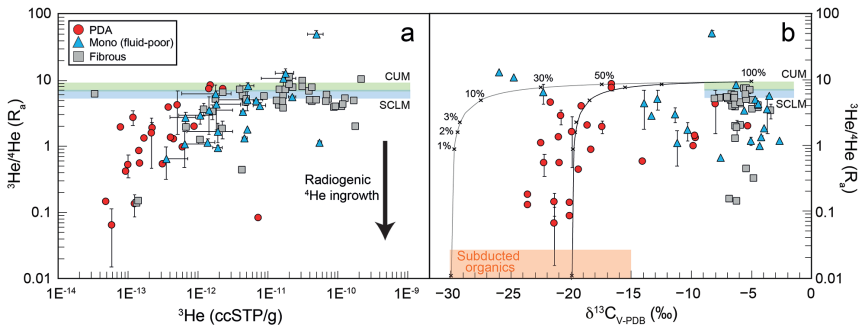


**Figure 5.** Helium isotope systematics of fluids released by in vacuo crushing and heating of PDAs, and monocrystalline and fibrous diamonds. The  $^3\text{He}/^4\text{He}$  and  $\delta^{13}\text{C}$  value of the modern convecting upper mantle (CUM) and the sub-continental lithospheric mantle (SCLM) are shown for reference (adapted from Mikhail et al. 2019a). The mixing lines shown in (a) are drawn between oceanic crustal-derived fluids with  $\delta^{13}\text{C} = -20$  and  $-30\text{‰}$ , and  $^3\text{He}/^4\text{He} = 0.01$  Ra, and mantle-derived fluids with  $\delta^{13}\text{C} = -5\text{‰}$  and  $^3\text{He}/^4\text{He} = 9$  Ra. The mixing lines plotted in (b) are hyperbolic as  $[\text{He}]_{\text{mantle}}/[\text{He}]_{\text{crust}}$  is assumed to be 10. Note, the mantle  $^3\text{He}/^4\text{He}$  endmember is slightly higher than the present-day upper asthenosphere and lithosphere mantle value, reflecting the U–Th decay-driven temporal evolution of  $^3\text{He}/^4\text{He}$  in the silicate Earth (Porcelli and Elliott 2008). Therefore, all  $^3\text{He}/^4\text{He}$  ratios are minimum values, although it appears that diamonds with  $>1 \times 10^{-12}$  ccSTP  $^3\text{He}/\text{g}$  are largely immune to the effect of ingrowth because the  $^4\text{He}$  production is too low to offset the R/Ra in this system (note the logarithmic scale of the x-axis). Comparative data are from Burgess et al. (1998), Gautheron et al. (2005), Broadley et al. (2018), Timmerman et al. (2018, 2019a, b), and Mikhail et al. (2019a).

After considering ingrowth of  $^4\text{He}$  due to the decay of U and Th in the sample it is clear that the PDAs and some monocrystalline diamonds characterized by low  $\delta^{13}\text{C}$  (commonly interpreted to indicate a crustal origin for the diamond-forming carbon), show high  $^3\text{He}/^4\text{He}$  ratios typical for mantle fluids (Gautheron et al. 2005; Mikhail et al. 2019a). The spread of data can be explained by mixing between a He-rich, high  $^3\text{He}/^4\text{He}$  mantle source with  $\delta^{13}\text{C} = -5\text{‰}$  and a He-poor, low  $^3\text{He}/^4\text{He}$  crustal component with  $\delta^{13}\text{C}$  between  $-15$  and  $-30\text{‰}$  (akin to the crustal organic carbon field in Fig. 3). The involvement of a crustal component is strongly supported by the  $^{15}\text{N}$ -enrichment in the  $^{13}\text{C}$ -depleted PDA samples and best matches either altered oceanic crust (Cartigny et al. 2014) or organic material hosted in sedimentary rocks (Thomazo et al. 2009). Hence, the He–C–N isotope systematics in PDAs could be described by mixing between fluids

released from subducted altered oceanic crust and mantle material, and mass balance skews the measured values towards the dominant component (Mikhail et al. 2019a). Therefore, although the  $^{13}\text{C}$ -depleted carbon and  $^{15}\text{N}$ -enriched nitrogen provide evidence for crustal sources for some of the PDA-forming fluids, the high  $^3\text{He}/^4\text{He}$  ratios in PDAs from Orapa reveal an unambiguous mantle component for these strongly  $^{13}\text{C}$ -depleted samples (Mikhail et al. 2019a).

In terms of PDA petrogenesis, these data characterize the PDA-forming metasomatic fluids as hybrids with subducted origins that have remobilized volatile elements in the subcratonic lithospheric mantle, initiated by subducted fluid percolating and interacting with potentially ancient material in the lithospheric mantle (first shown by Jacob et al. 2000).

### Nitrogen aggregation and mantle residence times

Nitrogen is the most abundant lattice-bound impurity in diamond. Over time, nitrogen defects as a function of temperature from single nitrogen atoms (C centers, Type Ib), to pairs of atoms (A centres, Type IaA), to 4 nitrogen atoms tetrahedrally arranged about a vacancy (B centres, Type IaB; Evans and Qi 1982). This sequence is quantified and expressed as the degree of nitrogen aggregation in %. The first step in this process (C to A centre aggregation) occurs quite rapidly while the second step (A to B centre) occurs much more slowly, where the exact rate of conversion depends on the temperature and nitrogen concentration (Chrenko et al. 1977). The A to B centre aggregation follows a second-order kinetics law (Evans and Qi 1982), meaning nitrogen aggregation can be used to estimate either the average temperature of residence or the duration of diamond residence in the mantle (assuming the other is known). Furthermore, platelets—planar interstitial carbon aggregates found on the {100} crystal planes—are the by-products of B centre formation and are prone to degradation during residence in the mantle (Woods 1986). The nitrogen aggregation data are fitted to a second-order kinetic model (e.g., Howell et al. 2012a, b) to ascertain information about the number, or depth, of the diamond-forming events.

As revealed by infrared spectroscopy, nitrogen aggregation states for PDAs span the whole spectrum from pure IaA to pure IaB (Mikhail et al. 2014c). Platelet characteristics are found to be regular, meaning they preserve their time-dependent history and have not been degraded by deformation and/or heating. There is no correlation between paragenesis (as defined by garnet geochemistry) and any of the IR characteristics for PDAs from Orapa (Mikhail et al. 2019b).

The nitrogen aggregation state for several diamond grains from individual PDA samples are homogeneous, in contrast with monocrystalline diamonds which can show highly variable nitrogen aggregation states between different growth zones reflecting multiple growth events (Boyd et al. 1987; Palot et al. 2013; Bulanova et al. 2014; Timmerman et al. 2017). Orapa PDAs show varying degrees of aggregation (10–76% B) and plot along calculated isotherms as a function of nitrogen abundance which can be fit to residence temperatures between 1100 and 1175 °C. However, the calculations of average mantle residence temperatures for PDAs in Mikhail et al. (2019b) assume residence time of 1000 m.y. (Fig. 6). The aggregation process is controlled less by time than it is by temperature, and if we reverse the calculation and vary temperature the reliability of these models is shown to be justifiably questionable. For example, if the model is computed with an elevated temperature of 1200 °C (increase of 25 °C from the maximum) or at 1400 °C (increase of 200 °C from the maximum), then the predicted mantle residence times for a sample with 76% B (and 600 ppm N) are 500 million years and 660,000 years, respectively.

Despite this, there is no evidence for higher-than-average residence temperatures (>1200 °C) for the Orapa PDAs, so the observation of regular and internally continuous nitrogen aggregation data (Mikhail et al. 2019b) means that the nitrogen aggregation data for each sample can be used to interpret their time–temperature history (with large uncertainties). Nevertheless, there are PDAs that show evidence for higher formation temperatures than 1200 °C, both at Orapa

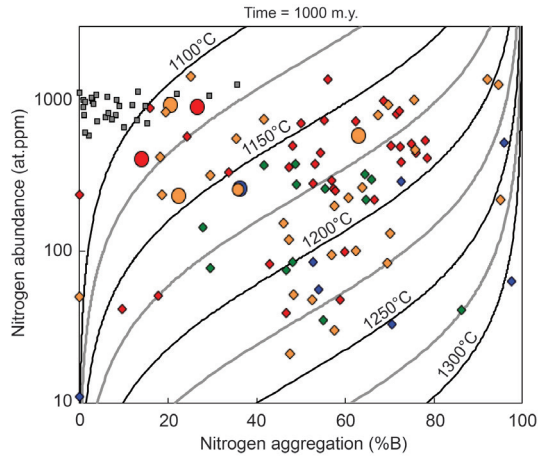


**Figure 6.** Variation diagrams for the average degree of nitrogen aggregation (%) vs. nitrogen abundance (at. ppm) for the diamonds from PDAs (**circles**) alongside the fibrous (**squares**) and monocrystalline diamonds (**diamonds**) from Orapa (adapted from Mikhail et al. 2019b). Isotherms chart the residence times of 1000 m.y. using the DiaMap software (Howell et al. 2012a, b). **Red** symbols—eclogitic paragenesis, **green**—peridotitic, **blue**—websteritic, **grey**—fibrous unknown, **orange**—unknown.

(Jacob et al. 2016) and also at Venetia, but nitrogen aggregation data unfortunately do not exist for these specific samples. One sample from the Venetia kimberlite, for example, was found to contain droplets of metallic iron and iron carbide and this assemblage requires temperatures above the liquidus of this system of 1370 °C at relevant pressures (Jacob et al. 2004).

All Orapa PDAs show B-centres of varying degrees, and this requires several hundred million years of residence in the mantle prior to emplacement in the crust at 91 Ma (Fig. 6). This is not the case for all PDAs, where data for PDAs of unknown provenance show nitrogen with very low and very high degrees of nitrogen aggregation (0–100% B; Mikhail et al. 2014c). These samples also show high temperature deformation and annealing structures in electron backscattered diffraction which perhaps could be argued to require significant mantle residence times (Rubanova et al. 2012). What can be stated, using these data, is that nitrogen aggregation data from PDA samples strongly oppose any notion that the carbon supersaturation event responsible for PDA-formation is temporally-associated with diamond-transporting kimberlite metasomatism (as has been proposed for fibrous samples; Boyd et al. 1994).

## INSIGHTS FROM THE GEOCHEMISTRY OF NON-DIAMOND COMPONENTS IN POLYCRYSTALLINE DIAMOND AGGREGATES

Geochemical and petrological studies of the non-diamond constituents are beset with technical challenges, many of them caused by the hardness anisotropy of diamond combined with the random orientation of the grains in PDAs and the high refractive index of diamond. For example, preparing PDAs for *in situ* microanalysis is exceedingly difficult due to the almost impossible task of producing adequately well-polished surfaces (Rubanova et al. 2012; Jacob et al. 2017). Similarly, the *ex situ* optical identification of the non-diamond phases or textural relationships is commonly obscured by the opaque nature of most PDAs (see Fig. 1)—the result of the many opaque impurities combined with the high optical refractivity of diamond. These challenges are intensified by the fact that the non-diamond phases, such as silicates, which hold a wealth of geochemical information, are present only in minor or trace amounts and can be heterogeneously distributed within a single sample (Mikhail et al.

2019b). To date, effective examination of the non-diamond phases in PDAs, such as garnet, requires mechanical disaggregation using a crusher which destroys all in situ petrographic data. For example, on some occasions, only after the mechanical extraction of the garnet did it transpire that a single PDA was host to multiple distinct populations of websteritic garnets, and even revealing garnets of different paragenesis within a single PDA, such as sample ORF53 from Orapa which was host to one purple (peridotitic) and one orange (websteritic) garnet (Mikhail et al. 2019b). This ‘lucky’ find of two very different garnets in one sample, in fact highlights a notable characteristic of the non-diamond components in PDAs, which is that they contain disequilibrium assemblages at grain-scale. Importantly, touching pairs of chemically homogeneous silicates of a single paragenesis (e.g., peridotitic–websteritic–eclogitic) as they are encountered in inclusions in monocrystalline diamond, are yet to be identified in PDAs.

Modern high-resolution computed tomography ( $\mu$ CT) offers an alternative and non-destructive method to optical microscopy and has occasionally been applied in PDAs (Fig. 2; Jacob et al. 2011; Logvinova et al. 2015). Multi-scale petrographic study of PDAs by  $\mu$ CT is still expensive but will most likely gain popularity with increasing access (i.e., supply vs. demand).

### Macro-inclusions and intergrowths

The most common non-diamond phases found in PDAs are garnets, followed by clinopyroxenes, but other phases can be present in significant abundances, including Mg-chromite, rutile, magnetite, sulphides and cohenite (iron carbide) (Gurney and Boyd 1982; Kirkley et al. 1991; Jacob et al. 2000, 2011, 2014, 2016; Dobosi and Kurat 2002, 2010; Mikhail et al. 2019b). Olivine and orthopyroxene are notably absent. Touching parageneses of silicate minerals are almost absent and often, PDAs host either only one mineral (most often garnet) or minerals of different parageneses which cannot have formed in equilibrium with each other. In addition, PDAs are known to display magnetism which requires the presence of magnetite and other magnetic phases (Jacob et al. 2011, 2016). It is worth pointing out that magnetite is a rare inclusion in PDAs, but its occurrence is more abundant in PDAs than in monocrystalline diamonds (Harris 1968; Sobolev et al. 1989) and may explain the magnetic properties of stewartite.

For diamond inclusions in general, garnet and clinopyroxene data are sub-divided into three groups, termed peridotitic, websteritic, and eclogitic, according to their silicate paragenesis. The assignment of inclusion paragenesis is empirical. For example, if assigned simply by color then websteritic garnets are sometimes wrongly classified as eclogitic, as both are orange, and indeed some workers have classified websteritic garnets as low-Ca eclogitic (e.g., Jacob et al. 2000; Kurat and Dobosi 2000). It is more accurate to use the major element geochemistry of garnet inclusions, such as the weight percent abundances of  $\text{Cr}_2\text{O}_3$  and CaO (Fig. 7a), where peridotitic are categorized by high-Cr and eclogitic garnets by low Cr- and high-Ca (Sobolev et al. 1973), and websteritic garnets are intermediate in composition (Gurney and Boyd 1982). The paragenetic distinction(s) for pyroxenes is less clear (Fig. 7b), where a peridotitic paragenesis is assigned for clinopyroxenes with Mg-number  $[(\text{Mg}/\text{Mg}+\text{Fe}) \times 100] > 85$ , Cr-number  $[(\text{Cr}/\text{Cr}+\text{Al}) \times 100] > 10$ , and  $< 2$  wt.%  $\text{Na}_2\text{O}$  (Aulbach et al. 2002). Alternatively, all garnet and clinopyroxene inclusions can be classified according to their endmember compositions (Fig. 7c, d).

This dataset shows that garnets in PDAs are most commonly websteritic, with peridotitic and eclogitic compositions less common for PDAs than as inclusions in monocrystalline diamond (Fig. 8a). Considering the available data (from Orapa, Venetia, Mirny, and unknown) we find that 57% of the garnets from PDAs are websteritic (Fig. 8a), compared with only 3% of worldwide monocrystalline diamond garnet inclusions (Stachel and Harris 2008; Fig. 8b). In contrast to the websteritic character of garnets in PDAs, the clinopyroxenes found in PDAs are most often peridotitic (79%; Fig. 8c), which contrasts with clinopyroxenes in monocrystalline diamond inclusions (18%; Fig. 8d). Whether the relative abundances or formation mechanisms for websteritic diamond inclusions represent pre-metasomatic mineralogical heterogeneity

in the upper mantle (Stachel and Harris 2008), eclogitic melt metasomatism (Aulbach et al. 2002; Kiseeva et al. 2016), or fluid metasomatism coeval with diamond formation (Mikhail et al. 2019b, 2021) is as yet unresolved. Characteristically, the most abundant mineral in the lithospheric mantle, olivine, is a notable absentee in PDAs. In addition, wehrlitic garnets and clinopyroxenes are absent, indicating that the striking absence of olivine is not a simple sampling bias, but is also reflected by the range of major element compositions for the silicates hosted in PDAs dominated by olivine-free websteritic/eclogitic parageneses (Figs. 7–8). The relatively high abundance of websteritic garnets in PDAs (Figs. 7–8) and the absence of olivine are a distinctive characteristic of PDAs that is not seen in the inclusion chemistry of monocrystalline diamonds from the same localities, such as Orapa (Mikhail et al. 2019b), or globally (Figs. 7–8), where peridotitic and eclogitic compositions represent the majority of the monocrystalline diamond yield (Figs. 7–8).

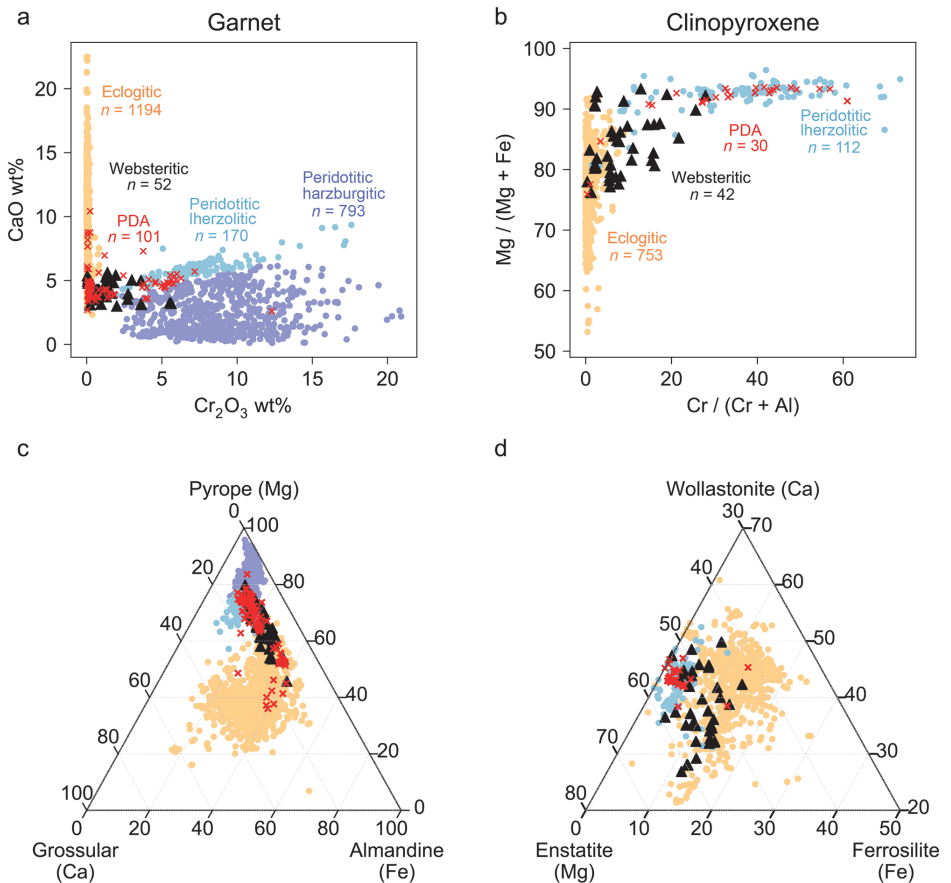


**Figure 7.** Inclusion parageneses and end-member compositions for garnets and clinopyroxenes from monocrystalline diamond and PDAs. The diamond inclusion database contains geochemical and metadata for > 9000 diamond inclusions. These plots utilize the clinopyroxene (*n* = 926), and garnet (*n* = 2628) data from lithospheric mantle diamonds. The data used here are sourced from Stachel and Harris (2008 and references therein) supplemented with more recent datasets (Viljoen et al. 1999; Cartigny et al. 2009; De Stefano et al. 2009; Hunt et al. 2009; Tappert et al. 2009; van Rythoven and Schulze 2009; Bulanova et al. 2010; Miller et al. 2014; Smith et al. 2016; Sobolev et al. 2016; Mikhail et al. 2019a; Jacob et al. unpublished).

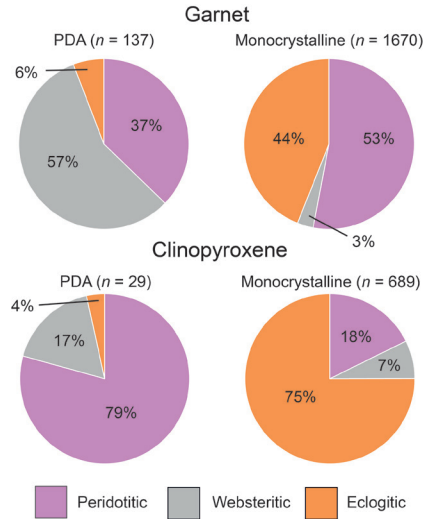


**Figure 8.** Pie charts reflecting the paragenesis for garnets (**left**) and clinopyroxenes (**right**) sourced from PDAs (**left**) and monocrystalline diamonds (**right**). The data for PDAs are sourced from Gurney and Boyd (1982), Gurney et al. (1984), Kirkley et al. (1995), Jacob et al. (2000, unpublished), Dobosi and Kurat (2010), Sobolev et al. (2016) and Mikhail et al. (2019a). The data for monocrystalline diamond inclusions are from Stachel and Harris (2008 and references therein).

### Trace elements and radiogenic isotopes of silicates in PDAs

Garnets intergrown with diamond in PDAs show typical chondrite-normalized rare earth element (REE) patterns with depleted LREE and relatively flat to convex-upward MREE to HREE (Fig. 9a–c). Peridotitic garnets have mildly sinusoidal patterns (Fig. 9a), similar to those included in monocrystalline diamonds (Stachel et al. 2004). Most of the websteritic garnets show no LREE enrichment and only some have mildly enriched LREE patterns (Fig. 9b), while this group has the highest HREE abundances of up to  $55 \times$  chondrite. Europium anomalies are not pronounced and, if present, are mostly within 15%, with one exception of a markedly positive Eu-anomaly (50%) in an eclogitic garnet from Orapa (ORF78, Mikhail et al. 2019b). Out of the four published trace element datasets for clinopyroxenes (Fig. 9d), two peridotitic samples (solid lines in Fig. 9d) have the highest REE abundances followed by a websteritic clinopyroxene (dotted line) and an omphacite (dashed line). Neither clinopyroxenes nor garnets show a correlation for REE abundances with their chromium content.

The notion for the involvement of ancient lithospheric material is provided by the unradiogenic  $^{87}\text{Sr}/^{86}\text{Sr}$  isotopic ratios (0.703189 to 0.703589) and unradiogenic Nd isotopic ratios of  $-15.9$  to  $-21.7$  ( $\epsilon_{\text{Nd}i}$ ) observed in four  $^{18}\text{O}$ -enriched websteritic garnet samples from  $^{13}\text{C}$ -depleted PDAs from Venetia (Jacob et al. 2000). These data fall towards the unradiogenic end of a large range of  $\epsilon_{\text{Nd}i}$  values for individually analysed peridotitic diamond inclusions from Venetia of  $-62$  to  $+157$  (Koornneef et al. 2017), and are typical for ancient lithospheric material.

### Micro-inclusions

While the release of detectable He, Ne, Ar and Xe after crushing of the PDAs under vacuum (Gautheron et al. 2005; Mikhail et al. 2019a) is circumstantial evidence for the presence of micro- to nano-fluid inclusions in PDAs, direct observation of small inclusions requires Focussed Ion Beam assisted Transmission Electron Microscopy (FIB-TEM) (Klein-BenDavid et al. 2006; Wirth 2009). For PDAs, these studies can relate minerals included in the diamond grains to those intergrown with them and thus can identify the type of metasomatic overprint in these rocks. A PDA from Orapa contained magnetite, pyrrhotite, rutile and

omphacite as micro-inclusions in the diamond grains. However, magnetite grains that were not fully encapsulated by diamond showed hematite and silicate alteration rims (Fig. 2; Jacob et al. 2011), whereas pyrrhotite grains were present only as micro-inclusions in diamonds and not as intergrown phases. This indicated a primary or even protogenetic nature of pyrrhotite and an unambiguous metasomatic overprint for the magnetites, thus highlighting the importance of recognising epigenetic changes in PDAs before petrological models are developed.

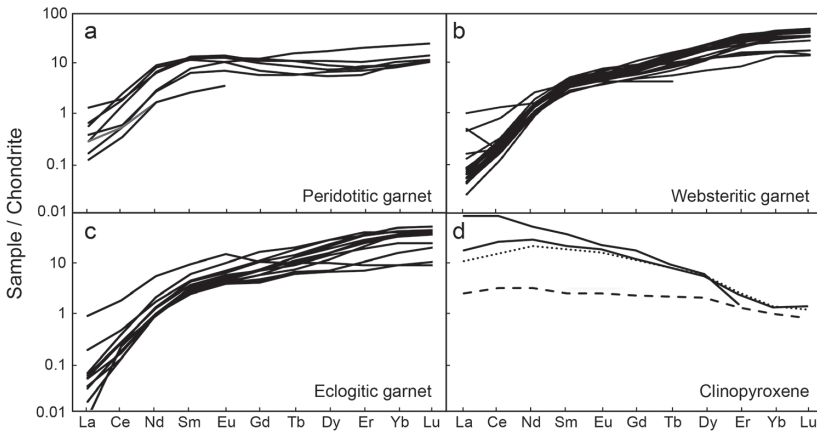


**Figure 9.** Chondrite-normalised rare earth element (REE) patterns for garnets (a–c) and clinopyroxenes (d) from PDAs. Different signatures in (d) denote peridotitic (solid lines), websteritic (dotted line) and eclogitic (dashed line) clinopyroxenes. Data from Jacob et al. (2000), Dobosi and Kurat (2010), Sobolev et al. (2016), and Mikhail et al. (2019b). Chondrite data from Sun and McDonough (1989).

Fluid inclusions in diamonds in this sample contained solid phases in the form of nanometre-sized grains of rutile, pyrrhotite and omphacites (but not magnetite), and silicic quenched phases (i.e., non-stoichiometric Si-bearing phases detected in cavities that formerly contained fluid. (Jacob et al. 2011). Diamond-related fluids worldwide range compositionally between four end-members, namely a saline fluid rich in Cl, K, Na, H<sub>2</sub>O and carbonate, a silicic end-member rich in Si, Al, K and H<sub>2</sub>O, high Mg- and low Mg-carbonatitic endmembers rich in Mg, Ca, Fe, K and carbonate, where both show continuous compositional arrays with the silicic endmember on a ternary diagram (Weiss et al. 2009, 2011). The PDA sample from Orapa contained a 10 nm-sized carbonate inclusion in addition to the silicic phases; hence, the diamond-related fluid composition in this sample is silicic and water-bearing with rare carbonates, while halides are absent. In the context of the general composition of diamond fluids worldwide (Weiss et al. 2022, this volume), these observations place this specific sample close to the silicic fluid endmember (Weiss et al. 2022, this volume). Based on these data, it could be hypothesized that fluid inclusions in PDAs have a compositional range similar to that found in other varieties of diamond, consistent with REE modelling of garnets (Mikhail et al. 2019b), but testing this hypothesis will have to await further direct observations in the future.

### Depth of origin

The scarcity of silicate inclusions (as opposed to silicate intergrowths) and the virtual absence of touching mineral phases in polycrystalline diamond aggregates has so far prevented attempts to derive a depth of formation for PDAs. Only one example is documented where a pressure estimate could be derived for the PDA from Orapa, described in *Micro-inclusions* above (Jacob et al. 2016). One of the pyrrhotite inclusions in diamond displayed a partially developed nanocrystalline reaction corona consisting of magnetite (Fig. 10).

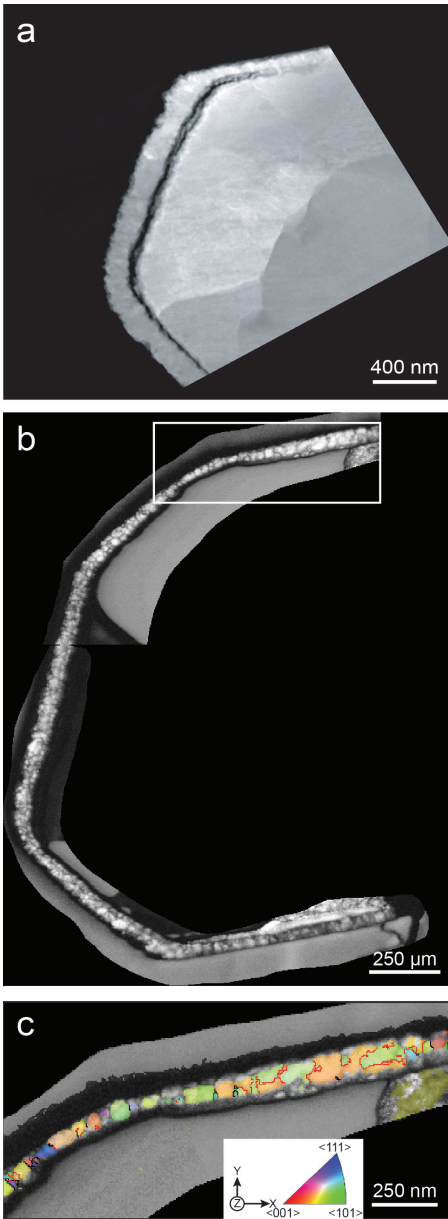


**Figure 10.** (a) TEM high angle annular dark field (HAADF) image of a diamond FIB foil showing a pyrrhotite inclusion with a magnetite rim. (b) Foreshooter electron image of the magnetite corona. (c) Crystal preferred orientation of magnetite in the area indicated by a **white rectangle** in (b) color-coded according to the legend and the reference frame (**bottom right**). Grain boundaries are in **black**, **red lines** are twin boundaries. Modified after Jacob et al. (2016).

Transmission Kikuchi Diffraction (TKD) established epitaxy between pyrrhotite, magnetite corona and diamond host, indicating that the diamond nucleated on the magnetite corona which, in turn, formed at the expense of pyrrhotite via a redox reaction with the carbon-bearing fluid. Further TKD analysis of the nanocrystalline magnetite corona revealed textural evidence, namely twinning, which is typical for phase transitions and similar to twinning observed in back reactions of a high-pressure assemblage of  $\text{Fe}_4\text{O}_5 + \text{Fe}_2\text{O}_3$  that replaces magnetite at pressures above 10–11 GPa at 1000–1600 °C (Schollenbruch et al. 2011; Woodland et al. 2012; Uenver-Thiele et al. 2017). The magnetite–( $\text{Fe}_4\text{O}_5 + \text{Fe}_2\text{O}_3$ ) phase boundary at ca. 10 GPa is thus a minimum pressure estimate for this sample, which must originate from ca. 320–330 km, close to the base of the Kaapvaal subcratonic lithosphere beneath the Orapa kimberlite cluster (Fouch et al. 2004).

Assuming no metasomatic overprinting for any of the PDA garnets, single garnet geobarometry performed using the machine learning-derived calibration of Thomson et al. (2021) yield average pressures of 6.0 (StDev  $\pm$  0.8) and 7.4 (StDev  $\pm$  0.5) GPa for peridotitic and websteritic garnets, respectively. The pressures for peridotitic and websteritic garnets were calculated using high and low Cr-calibration for P-type and E/W-type garnets from (Wijbrans et al. 2016). However, corresponding pressures calculated for samples containing multiple garnets yield pressure differences up to  $\pm 2$  GPa, which could be explained by metasomatic overprinting for one of the garnets at an undefined time after diamond formation. These differences in pressure, however, also call into question the reliability of using single garnet geobarometry for PDAs without knowing if the garnets have been isolated or exposed to the mantle since PDA formation. In addition, the total fraction majorite content (i.e., Si-excess and considering Mj + NaMj) for garnets in PDAs shows a maximum of 0.06 with an average of only 0.01 ( $n = 104$ ). Therefore, we find no evidence to support the notion that PDAs, as a group, are sourced from depths of below the subcratonic lithosphere.

### Constraints on the formation age(s) of PDAs

There are no *bona fide* formation ages for PDAs, as yet. However, the preservation of significant trace element zonation in PDA-hosted garnets from Venetia (South Africa; Fig. 11) requires that these samples precipitated shortly before kimberlite eruption, based on modelling the trace element heterogeneity using known diffusion coefficients (Jacob et al. 2000). In addition, these same garnets show strongly unradiogenic  $\epsilon_{\text{Nd}}$  with values from  $-15.9$  to  $-21.7$   $\epsilon_{\text{Nd}}$  (see above), typical for ancient lithospheric material, which was used to argue for recent remobilization of this material upon the formation of PDAs at Venetia (Jacob et al. 2000). Therefore, this means that the garnets contain older lithospheric material remobilized with the diamond-forming fluid at Venetia. In contrast, garnets from Orapa PDAs show very little, if any trace element variability within single garnets (Mikhail et al. 2019b). The geochemistry of garnets from Orapa PDAs therefore provides no evidence of a young formation age and no reliable evidence for a metasomatic event around the time of emplacement at 91 Ma (Mikhail et al. 2019b), in agreement with the nitrogen aggregation results for the diamonds hosting these garnets (discussed earlier).

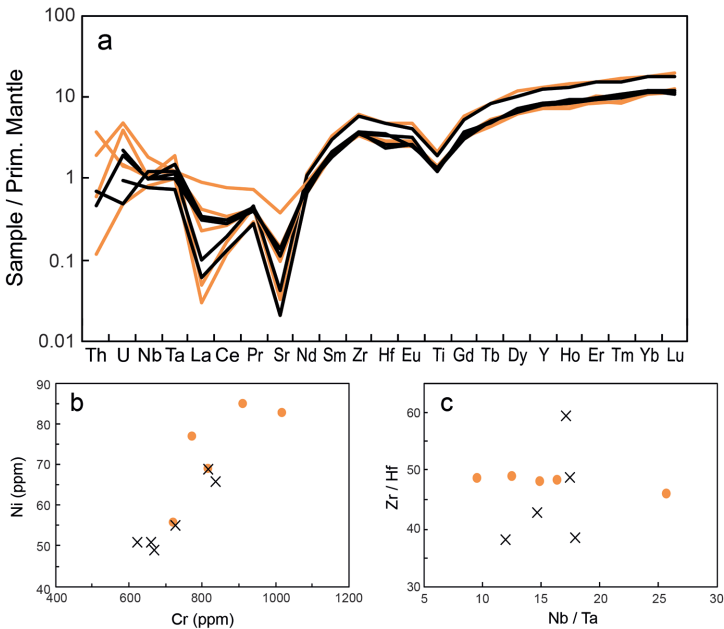


**Figure 11.** Trace element zonation in three different grains of websteritic garnet in PDA from Venetia (sample V948, Jacob et al. 2000). (a) Spidergrams (normalized to primitive mantle: Sun and McDonough 1989) show significant differences in most elements apart from titanium and the mid and heavy REE in the grains. (b) compatible element Ni and Cr variations (**crosses**: grain averages, **orange** are zones in two different grains), (c) variations in Nb/Ta and Zr/Hf ratios in the zoned grains.

### Oxidation State

Polycrystalline diamond aggregates are broadly similar to subcratonic lithospheric monocrystalline diamonds with respect to the chemistry of the minerals included in and intergrown with the diamond grains. Like monocrystalline diamonds, PDAs span a large range of ca. 7 log units in oxygen fugacity ( $fO_2$ ) as evidenced by their associated minerals: carbonates and magnetite in PDAs from Orapa indicate oxidising conditions of around  $\log fO_2 = -6$  (Jacob et al. 2011), while cohenite (iron-carbide) as well as native iron in PDAs

from Venetia record distinctly reducing conditions of about  $\log fO_2 = -13$  (Jacob et al. 2004, 2016); this characteristic reducing signature is shared with the monocrystalline diamond suite at this locality (Deines et al. 2001).

Redox reactions, involving redox couples of carbon-bearing fluids and Fe–Ni-bearing phases, are proposed to be major diamond formation processes in the deep Earth's mantle (Rohrbach and Schmidt 2011). PDAs have delivered the first direct evidence for redox freezing of diamond by reduction of carbonatitic fluids with pyrrhotite to form magnetite and diamond (Jacob et al. 2016), while native iron and iron carbide (cohenite) included in a websteritic garnet (Jacob et al. 2004) are products of oxidation of a methane-bearing fluid. It should however be noted, that as of yet, the relationship between monocrystalline diamonds and polycrystalline diamond aggregates is unknown. Since the database for PDAs is much smaller than for monocrystalline diamonds, it is difficult to evaluate the abundance and potential prevalence of certain oxidation states, but the large range of  $fO_2$  is significant and suggests a prominent role of redox gradients and transient, small-scale equilibria in their formation. Grain-scale equilibrium, instead, is scarce and most often absent in PDAs.

## OVERVIEW OF CURRENT UNDERSTANDING FOR POLYCRYSTALLINE DIAMOND FORMATION

There can be no single model for polycrystalline diamond-formation, just like there is no single model for monocrystalline diamond-formation. For example, no single model can explain why some samples show high- and low- nitrogen aggregation (Mikhail et al. 2014c, 2019b) and no single model can reconcile the range of oxygen fugacities required to stabilize carbonates + magnetite at Orapa (Jacob et al. 2011, 2016) and cohenite + native iron at Venetia (Jacob et al. 2004).

The mineral inclusions and intergrowths show no indication for derivation from depths well below the subcratonic lithosphere, unlike some monocrystalline diamonds. Only one sample has yet allowed a reliable determination of a depth of formation, placing it close to the base of the subcratonic lithosphere of the Kaapvaal craton at the Orapa locality (Jacob et al. 2016), determined to be at 320–330 km by Fouch et al. (2004). This depth of origin, combined with the absence of significant Si-excess in the garnets, may mean that these diamond species primarily consist of remobilized material derived from the carbonate-enriched keels of the subcratonic lithosphere (Jacob et al. 2000; Foley 2009) and/or that carbon-rich fluids from depth reacted and formed diamond upon entering the ductile to brittle deformation transition zone at the base of the subcratonic lithospheric mantle as suggested by Jacob et al. (2004). The fact that PDAs have only been reported from plume-related Group I kimberlites and not from Group II kimberlites that originate from subcratonic lithospheric sources (Le Roux et al. 2003; Becker and Le Roux 2006) agrees well with the depth of derivation for the PDAs from the base of the lithosphere. What is most apparent is that some form of chemical interaction is involved between surface and mantle material, where mixing between subducted crustal material, namely altered oceanic crust, with ambient mantle carbon and the subcratonic lithospheric mantle is strongly supported by major, minor, and trace element systematics, as well as several isotopic systems (He–C–N–O–Sr–Nd) acquired carbon, oxides, and silicates in the PDAs.

Most garnets in PDAs are websteritic, but the clinopyroxenes are mostly peridotitic (Figs. 7–8). The predominance of websteritic garnets in PDAs (Figs. 7–8) and the absence of olivine (and of orthopyroxene) are a distinctive characteristic of PDAs that are not seen in the inclusion chemistry of monocrystalline diamonds (Figs. 7–8). Subcratonic garnet websterites are typically products of melt interaction with mantle rocks (e.g., Rehfeldt et al. 2008; Mallik and Dasgupta 2012). Hence, the websteritic silicates in the PDAs are most likely hybrid phases and are, like the magnetites, reaction products of the interactions of the carbon-bearing

fluid with surrounding mantle material upon diamond formation. For example, a recent study used a predictive thermodynamic modelling approach and was able to fit the major element compositions websteritic garnet and clinopyroxenes for a large number of PDAs, and also those from monocrystalline diamonds (Mikhail et al. 2021). This predictive thermodynamic model was run using the extended Deep Earth Water model (Huang and Sverjensky 2019), which enables the assessment of a huge range of variables ( $P$ – $T$ – $X$ ). The model produces a reaction pathway resulting from the reaction of an eclogitic fluid with a range of model peridotites (lherzolite, harzburgite, and dunite) at 5 GPa, 1000 °C, and across a range of redox conditions ( $\log fO_2 = -1$  to  $-6$ ). The outputs include the co-evolution for fluid composition (including  $fO_2$  and pH) alongside carbon speciation under isothermal and isobaric conditions, and the major element composition and modal abundances for the precipitates (silicates and oxides in the case of Mikhail et al. 2021). The model does not encompass all conditions and compositions observed in nature—it is S- and Cr-free, limited to at 5 GPa and 1000 °C and adopts a smaller range of  $fO_2$  than observed for PDAs—but it does satisfy a range of features common to all PDAs: Mikhail et al. (2021) show that fluid–rock interaction can result in the formation of (high-Mg) eclogitic, websteritic, and peridotitic garnets and clinopyroxenes from a single fluid during a diamond-forming metasomatic reaction (Fig. 12).

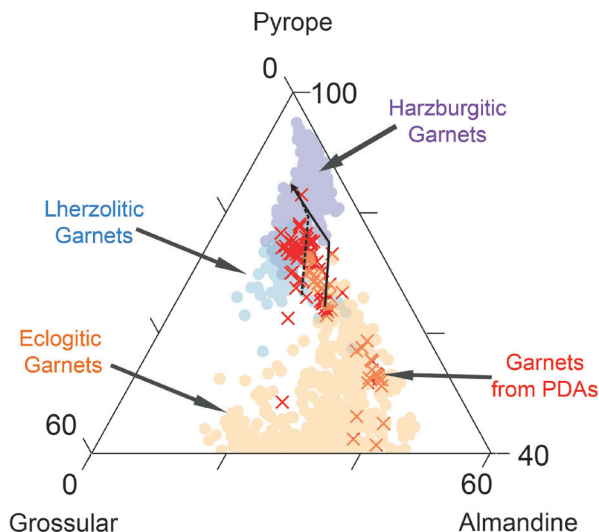


**Figure 12.** Selected model results for predicted garnet compositions during progressive metasomatism and diamond formation at 5 GPa and 1000 °C. The lines for the runs plotted are thick enough to represent the average trajectories for an eclogitic fluid reacting with model peridotites (lherzolite, harzburgite, and dunite) and model peridotites (lherzolite, harzburgite, and dunite) + aragonite (**dashed line**). Data are from Mikhail et al. (2021) and the input and output files are available at <https://doi.org/10.17630/32ebd3c0-bba6-4aa1-9b6d-c53a0a3b61e0>. All comparative data shown are taken from the same sources as listed in the caption of Figure 7c.

Interestingly, most models generate ca. 2% by volume magnetite, which could speak to the formation of stewartite, and because the model also generated websteritic garnets (predominantly), this might speak to the formation of framesite (Fig. 12). The model in Mikhail et al. (2021) would remobilize ancient material via dissolution in the fluid and re-precipitate diamond + silicates + oxides (Jacob et al. 2000). This model of diamond growth progressively trapping material during a reaction pathway could also satisfy the occurrence of chemical zonation in PDAs (Fig. 4) and the fact that some PDAs host disequilibrium

assemblages (i.e., mixed paragenesis) because the diamond-, silicate-, and oxide-forming fluid follows an evolving pathway. For garnets this would be from low pyrope–eclogitic to high pyrope–peridotitic (Fig. 12). This would provide the mechanism to preserve snapshots of the metasomatic reaction by occasionally trapping garnets and clinopyroxenes at different stages of the reaction thus forming a diamond with inclusions of mixed paragenesis in the same place (no mechanically challenging spatial mobility is required to explain the occurrence) and during the same metasomatic event.

Noteworthy, PDAs also contain protogenetic and epigenetic phases in addition to syngenetic phases which highlights the need for petrographically contextualized data (e.g.,  $\mu$ CT datasets). However, the timing of PDA formation is currently the least constrained aspect of their story, and one of the most integral to any realistic geological model. Several lines of evidence discussed in the sections above support the notion that some PDAs are geologically ‘old’ while others are ‘young’ in relation to kimberlite emplacement, hence pointing to episodic formation of PDAs likely linked to large-scale geodynamic events. Ergo, we are confident to say that PDA-formation is dynamic and usually involves the tectonically-induced chemical disequilibrium and fluid metasomatism at the base of the SCLM following the interaction of indigenous and subducted carbonaceous material. But we find no evidence for a single model for polycrystalline diamond-formation (note, the model of Mikhail et al. 2021 does not fit the low-Mg eclogitic PDAs). Excitingly, these data also suggest that there is no single polycrystalline diamond-forming event, globally.

## PERSPECTIVES ON FUTURE RESEARCH

Placing diamond formation into the context of large-scale tectonothermal processes, such as subduction and plume–lithosphere interaction, is a fundamental requirement for understanding the deep carbon cycle. Therefore, placing PDA formation into the context of diamond formation is essential. This review has outlined what we know and exposed some glaring gaps in the knowledge base. Some of the most pressing questions focus on the what, when, and how of PDA formation.

### When did PDAs form?

The temporal relationship between the PDAs and other diamond types, and their host kimberlites, requires immediate attention. While recent instrumental developments have brought radiogenic isotope analysis of very small samples within reach (Koorneef et al. 2014), we do not currently have any direct age information for PDAs. Circumstantial evidence from preserved trace element zonation (Fig. 11) and nitrogen aggregation point to young ages for some samples, whereas mantle residence times for other PDAs are required to be long to explain their nitrogen aggregation characteristics (Fig. 6). PDA formation could be as dynamic as monocrystalline diamond formation with episodic formation spanning billions of years (Gurney et al. 2010; Timmerman et al. 2017), or they could result from distinct metasomatic event(s) which may or may not be related to the formation of monocrystalline diamonds at specific localities (Mikhail et al. 2019b).

### What formed PDAs?

The geochemistry of fluids for Orapa PDAs has been calculated using REE data from garnets and these data fit a model for a fluid geochemistry intermediate between the saline and carbonate endmembers (Mikhail et al. 2019b). Direct observations of the fluids by TEM in PDAs from Venetia instead showed carbonatitic-silicic chemistry (Jacob et al. 2014). More *in situ* analyses of the sub-micron fluid inclusions are required to quantify their major and minor element geochemistry to accurately chart their geochemistry within the established framework of the saline-silicic-carbonatitic ternary system (see Weiss et al. 2022, this volume).

### How do PDAs form?

The source of PDA-forming fluids is variable and complex, of this there is no doubt. What is clear is that the source materials show mantle and crustal geochemical and isotopic signatures (Figs. 3, 4, 5), and the websteritic silicates are products of wallrock-fluid reactions (Mikhail et al. 2021). This requires some degree of mechanical exchange by subduction zone plate tectonics. However, the isotopic range of C–N data reveal that some PDAs form in distinct episodes with distinct isotopic sources. These data are recorded by spatially unconstrained stepped combustion (Mikhail et al. 2014a), but spatially resolved to be in the order of < 20 mm using SIMS data for some samples (Fig. 4). It is unclear, however, on which time scales these diamond-forming events were recorded in this particular sample suite. It is also unclear how widespread element and isotope zonation is within PDAs, both in the diamond grains (Fig. 4) as well as in the silicates (Fig. 11) because of the difficulty in polishing flat surfaces required to map out zonation using CL imaging or SIMS or LA-ICPMS profiling. Further elucidation of the processes and timescales that lead to the formation of this species of diamond carries the potential to provide an important different perspective into the deep carbon cycle and link global geotectonic processes with the redox-freezing of carbon in the deep lithosphere.

### ACKNOWLEDGMENTS

The authors are grateful for reviews by Peter J. Heaney, Oded Navon and Tom McCandless. Karen Smit and Steve Shirey are thanked for their smooth editorial handling and support. DEJ acknowledges financial support by the German Sciences Foundation and the Australian Research Council (CE110001017). SM acknowledges financial support by a National Environmental Research Council standard grant (NE/PO12167/1) and a UK Space Agency Aurora grant (ST/T001763/1).

### REFERENCES

- Aulbach S, Stachel T, Viljoen KS, Brey GP, Harris JW (2002) Eclogitic and websteritic diamond sources beneath the Limpopo Belt—is slab-melting the link? *Contrib Mineral Petrol* 143:143–156
- Becker M, Le Roux AP (2006) Geochemistry of South African on- and off-craton, Group I and Group II kimberlites: petrogenesis and source region evolution. *J Petrol* 47:673–703
- Boyd SR, Pillinger CT (1994) A preliminary study of  $^{15}\text{N}/^{14}\text{N}$  in octahedral growth form diamonds. *Chem Geol* 116:43–59
- Boyd SR, Mathey DP, Pillinger CT, Milledge HJ, Mendelsohn M, Seal M (1987) Multiple growth events during diamond genesis: an integrated study of carbon and nitrogen isotopes and nitrogen aggregation state in coated stones. *Earth Planet Sci Lett* 86:341–353
- Boyd SR, Pillinger CT, Milledge HJ, Seal MJ (1992) C and N isotopic composition and the infrared absorption spectra of coated diamonds: evidence for the regional uniformity of  $\text{CO}_2$ – $\text{H}_2\text{O}$  rich fluids in lithospheric mantle. *Earth Planet Sci Lett* 108:139–150
- Boyd SR, Pineau F, Javoy M (1994) Modelling the growth of natural diamonds. *Chem Geol* 116:29–42
- Broadley MW, Kagi H, Burgess R, Zedgenizov D, Mikhail S, Imayrac M, Ragozin A, Pomazansky B, Sumino B (2018) Plume–lithosphere interaction, and the formation of fibrous diamonds. *Geochem Perspect Lett* 8:26–30
- Brooker R, Du Z, Blundy JD, Keley SP, Allan NL, Wood BJ, Chamorro EM, Wartho JA, Purton JA (2003) The ‘zero charge’ partitioning behaviour of noble gases during mantle melting. *Nature* 432:738–741
- Bulanova G, Walter M, Smith C, Kohn S, Armstrong L, Blundy J, Gobbo L (2010) Mineral inclusions in sublithospheric diamonds from Collier 4 kimberlite pipe, Juina, Brazil: subducted protoliths, carbonated melts and primary kimberlite magmatism. *Contrib Mineral Petrol* 160:489–510
- Bulanova GP, Wiggers de Vries D, Mikhail S, Beard A, Davies GR, Pearson DG (2014) Carbon recycling and polygenetic origin of eclogitic diamonds recorded by a single crystal from the Mir pipe (Yakutia). *Chem Geol* 381:40–55
- Burgess R, Johnson L, Mathey D, Harris J, Turner G (1998) He, Ar and C isotopes in coated and polycrystalline diamonds. *Chem Geol* 146:205–217
- Busigny V, Cartigny P, Laverne C, Teagle D, Bonifacie M, Agrinier P (2019) A re-assessment of the nitrogen geochemical behaviour in upper oceanic crust from Hole 504B: Implications for subduction budget in Central America. *Earth Planet Sci Lett* 525:115735
- Cartigny P (2005) Stable isotopes and the origin of diamond. *Elements* 1:79–84

- Cartigny P (2010) Mantle-related carbonados? Geochemical insights from diamonds from the Dachine komatiite (French Guiana). *Earth Planet Sci Lett* 296:329–339
- Cartigny P, Boyd SR, Harris JW, Javoy M (1997) Nitrogen isotopes in peridotitic diamonds from Fuxian, China: the mantle signature. *Terra Nova* 9:175–179
- Cartigny P, Harris JW, Javoy M (1998a) Eclogitic diamond formation at Jwaneng: no room for a recycled component. *Science* 280:1421–1424
- Cartigny P, Harris JW, Phillips D, Girard M, Javoy M (1998b) Subduction-related diamonds? The evidence for a mantle-derived origin from coupled  $\delta^{13}\text{C}$ – $\delta^{15}\text{N}$  determinations. *Chem Geol* 147:147–159
- Cartigny P, Harris JW, Javoy M (1999) Eclogitic, peridotitic and metamorphic diamonds and the problems of carbon recycling—the case of Orapa (Botswana). 7<sup>th</sup> International Kimberlite Conference Extended Abstracts, p 117–124
- Cartigny P, Stachel T, Harris JW, Javoy M (2004) Constraining diamond metasomatic growth using C- and N-stable isotopes: examples from Namibia. *Lithos* 77:359–373
- Cartigny P, Farquhar J, Thomassot E, Harris JW, Wing B, Masterson A, McKeegan K, Stachel T (2009) A mantle origin for Paleoproterozoic peridotitic diamonds from the Panda kimberlite, Slave Craton: evidence from  $^{13}\text{C}$ -,  $^{15}\text{N}$ - and  $^{33,34}\text{S}$  stable isotope systematics. *Lithos* 112:852–864
- Cartigny P, Palot M, Thomassot E, Harris JW (2014) Diamond formation: a stable isotope perspective. *Annu Rev Earth Planet Sci* 42:699–732
- Chacko T, Cole DR, Horita J (2001) Equilibrium oxygen, hydrogen and carbon isotope fractionation factors applicable to geologic systems. *Rev Mineral Geochem* 43:1–81
- Chrenko RM, Tuft RE, Strong HM (1977) Transformation of state of nitrogen in diamond. *Nature* 270:141–144
- De Stefano A, Kopylova MG, Cartigny P, Afanasiev V (2009) Diamonds and eclogites of the Jericho kimberlite (Northern Canada). *Contrib Mineral Petrol* 158:295–315
- De Waele B, Johnson SP, Pisarevsky SA (2008) Palaeoproterozoic to Neoproterozoic growth and evolution of the eastern Congo Craton: Its role in the Rodinia puzzle. *Precambrian Res* 160:127–141
- Deines P (1980) The carbon isotopic composition of diamonds: relationship to diamond shape, color, occurrence and vapor composition. *Geochim Cosmochim Acta* 44:943–961
- Deines P, Viljoen F, Harris JW (2001) Implications of the carbon isotope and mineral inclusion record for the formation of diamonds in the mantle underlying a mobile belt: Venetia, South Africa. *Geochim Cosmochim Acta* 65:813–838
- Dobosi G, Kurat G (2002) Trace element abundances in garnets and clinopyroxenes from diamondites—a signature of carbonatitic fluid. *Mineral Petrol* 76:21–38
- Dobosi G, Kurat G (2010) On the origin of silicate-bearing diamondites. *Mineral Petrol* 99:29–42
- Evans T, Qi Z (1982) The kinetics of the aggregation of nitrogen atoms in diamond. *Proc R Soc A* 381:159–178
- Fettke CR, Sturges FC (1933) Note on the structure of carbonado or black diamond. *Am Mineral* 18:172–174
- Foley SF (2009) Rejuvenation and erosion of the cratonic lithosphere. *Nat Geosci* 1:503–510
- Fouch MJ, James DE, VanDecar JC, van der Lee S, and Kaapvaal Seismic Group (2004) Mantle seismic structure beneath the Kaapvaal and Zimbabwe cratons. *S Afr J Geol* 107:33–44
- Fourel F, Lécuyer C, Demeny A, Boulvais P, Lange L, Jacob DE, Kovacs I (2017)  $^2\text{H}/^1\text{H}$  measurements of amphiboles and nominally anhydrous minerals (clinopyroxene, garnet and diamond) using high-temperature CF-EA-PY-IRMS. *Rapid Commun Mass Spectrom* 31:2066–2072
- Gautheron C, Cartigny P, Moreira M, Harris JW, Allegre CJ (2005) Evidence for a mantle component shown by rare gases, C and N isotopes in polycrystalline diamonds from Orapa (Botswana). *Earth Planet Sci Lett* 240:559–572
- Gurney JJ, Boyd FR (1982) Mineral intergrowths with polycrystalline diamonds from the Orapa Mine, Botswana. *Carnegie Institution Yearbook*, p 267–273
- Gurney JJ, Harris JW, Rickard RS (1984) Silicate and oxide inclusions in diamonds from the Orapa Mine, Botswana. *In: Kimberlites II: The mantle and crust–mantle relationships*. Vol. 2 Elsevier, p 3–9
- Gurney JJ, Helmstaedt HH, Richardson SH, Shirey SB (2010) Diamonds through time. *Econ Geol* 105:689–712
- Haggerty SE (1999) A diamond trilogy: Superplumes, supercontinents, and supernovae. *Science* 285:851–860
- Haggerty SE (2014) Carbonado: Physical and chemical properties, a critical evaluation of proposed origins, and a revised genetic model. *Earth Sci Rev* 130:49–72
- Haggerty SE (2017) Carbonado diamond: A review of properties and origin. *Gems Gemol* 53:168–172
- Halama R, Bebout GE, John T, Schenk V (2010) Nitrogen recycling in subducted oceanic lithosphere: the record in high- and ultrahigh-pressure metabasaltic rocks. *Geochim Cosmochim Acta* 74:1636–1652
- Halama R, Bebout GE, John T, Scambelluri M (2014) Nitrogen recycling in subducted mantle rocks and implications for the global nitrogen cycle. *Int J Earth Sci* 103:2081–2099
- Harris JW (1968) The recognition of diamond inclusions. *Industrial Diamond Review*. DeBeers Industrial Diamond Division
- Heaney PJ, Vicenzi EP, De S (2005) Strange diamonds: the mysterious origins of carbonado and framesite. *Elements* 1:85–89
- Hoefs J (2009) *Stable Isotope Geochemistry*. Springer, New York
- Howell D, O'Neill CJ, Grant KJ, Griffin WL, O'Reilly SY, Pearson NJ, Stern RA, Stachel T (2012a) Platelet development in cuboid diamonds: insights from micro-FTIR mapping. *Contrib Mineral Petrol* 164:1011–1025
- Howell D, O'Neill CJ, Grant KJ, Griffin WL, Pearson NJ, O'Reilly SY (2012b)  $\mu$ -FTIR mapping: distribution of impurities in different types of diamond growth. *Diamond Relat Mater* 29:29–36

- Huang F, Sverjensky DA (2019) Extended Deep Earth Water Model for predicting major element mantle metasomatism. *Geochim Cosmochim Acta* 254:192–230
- Hunt L, Stachel T, Morton R, Grüttler H, Creaser RA (2009) The Carolina kimberlite, Brazil—Insights into an unconventional diamond deposit. *Lithos* 112:843–851
- Jackson CRM, Parman SW, Kelley SP, Cooper RF (2013) Constraints on light noble gas partitioning at the conditions of spinel-peridotite melting. *Earth Planet Sci Lett* 384:178–187
- Jacob DE, Viljoen KS, Grassineau N, Jagoutz E (2000) Remobilization in the cratonic lithosphere recorded in polycrystalline diamond. *Science* 289:1182–1185
- Jacob DE, Kronz A, Viljoen KS (2004) Cohenite and native iron inclusions in garnets from polycrystalline diamonds. *Contrib Mineral Petrol* 146:566–576
- Jacob DE, Wirth R, Enzmann F, Kronz A, Schreiber A (2011) Nano-inclusion suite and High Resolution Micro-Computed-Tomography of polycrystalline diamond (framesite) from Orapa, Botswana. *Earth Planet Sci Lett* 308:307–316
- Jacob DE, Dobrzynetskaia L, Wirth R (2014) New insight into polycrystalline diamond genesis from modern nanoanalytical techniques. *Earth Sci Rev* 136:21–35
- Jacob DE, Piazzolo S, Schreiber A, Trimby P (2016) Redox-freezing and nucleation of diamond via magnetite formation in the Earth's mantle. *Nat Commun* 7:11891
- Jacob DE, Stern RA, Chapman J, Piazzolo S (2017) Insights into diamond formation from polycrystalline diamond aggregates. *Goldschmidt Abstracts* #1801
- Javoy M, Pineau F, Delorme H (1986) Carbon and nitrogen isotopes in the mantle. *Chem Geol* 57:41–62
- Kaminsky FV, Galimov EM, Genshaft YS, Ivanovskaya IN, Klyuev YA, Rovsha VS, Sandomirskaya SM, Smirnov VI (1981) Boart with a garnet from the Mir pipe (Yakutia). *Doklady Akademii Nauk SSSR* 256:674–677
- Kirkley MB, Gurney JJ, Otter ML, Hill SJ, Daniels LR (1991) The application of C isotope measurements to the identification of the sources of C in diamonds: a review. *Appl Geochem* 6:477–494
- Kirkley MB, Gurney JJ, Rickard RS (1995) Jwaneng Framesites: Carbon isotopes and intergrowth compositions. *In: Diamonds: characterization, genesis and exploration*. Meyer HOA, Leonardos OH (eds.) CPRM Spec Publ, Sao Paolo, p 127–135
- Kiseeva ES, Wood BJ, Ghosh S, Stachel T (2016) The pyroxenite - diamond connection. *Geochem Perspect Lett* 2:1–9
- Klein-BenDavid O, Wirth R, Navon O (2006) TEM imaging and analysis of microinclusions in diamonds: a close look at diamond-growing fluids. *Am Mineral* 91:353–365
- Klein-BenDavid O, Pearson DG, Nowell GM, Ottley C, McNeill JCR, Cartigny P (2010) Mixed fluid sources involved in diamond growth constrained by Sr–Nd–Pb–C–N isotopes and trace elements. *Earth Planet Sci Lett* 289:123–133
- Koga KT, van Orman JA, Walter MJ (2003) Diffusive relaxation of carbon and nitrogen isotope heterogeneity in diamond: a new thermochronometer. *Phys Earth Planet Sci* 139:35–43
- Koornneef JM, Bouman C, Schwieters JB, Davies GR (2014) Measurement of small ion beams by thermal ionisation mass spectrometry using new  $10^{13}$  Ohm resistors. *Anal Chimica Acta* 819:49–55
- Koornneef JM, Gress MU, Chinn IL, Jelsma HA, Harris JW, Davies GR (2017) Archaean and Proterozoic diamond growth from contrasting styles of large-scale magmatism. *Nat Commun* 8:648
- Kurat G, Dobosi G (2000) Garnet and diopside-bearing diamondites (framesites). *Mineral Petrol* 69:142–159
- Le Roux AP, Bell DR, Davis P (2003) Petrogenesis of Group I kimberlites from Kimberley, South Africa: evidence from bulk-rock geochemistry. *J Petrol* 44:2261–2286
- Leonardos OH (1937) Diamante e carbonado no estado da Bahia. *Metallurgia servio de fomento da producao Mineral* 19:1–23
- Logvinova AM, Taylor LA, Fedorova EN, Yeliseyev AP, Wirth R, Howarth G, Reutsky VN, Sobolev NV (2015) A unique diamondiferous peridotite xenolith from Udachnaya kimberlite pipe, Yakutia: role of subduction in diamond formation. *Russ Geol Geophys* 56:306–320
- Mallik A, Dasgupta R (2012) Reaction between MORB-eclogite derived melts and fertile peridotite and generation of ocean island basalts. *Earth Planet Sci Lett* 329–330:97–108
- Maruoka T, Kurat G, Dobosi G, Koerberl C (2004) Isotopic composition of carbon in diamondites: record of mass fractionation in the upper mantle. *Geochim Cosmochim Acta* 68:1635–1644
- Mattey DP, MacPherson CG (1993) High-precision oxygen isotope microanalysis of ferromagnesian minerals by laser-fluorination. *Chem Geol (Isotope Geosci Sect)* 105:305–318
- McCandless TE, Kirkley MB, Robinson DN, Gurney JJ, Griffin WL, Cousens DR, Boyd FR (1989) Some initial observations on polycrystalline diamonds mainly from Orapa. *Extended Abstracts 28<sup>th</sup> Int Geol Congr*, p 47–51
- Mikhail S, Howell D (2016) A petrological assessment of diamond as a recorder of the mantle nitrogen cycle. *Am Mineral* 101:780–787
- Mikhail S, Kurat G, Verchovsky AB, Jones AP (2013) Peridotitic and websteritic diamondites provide new information regarding mantle melting and metasomatism induced through subduction of crustal volatiles. *Geochim Cosmochim Acta* 107:1–11
- Mikhail S, Howell D, Hutchison MT, Verchovsky AB, Warburton P, Southworth R, Thompson AR, Jones AP, Milledge HJ (2014a) Constraining the internal variability of the stable isotopes of carbon and nitrogen within mantle diamonds. *Chem Geol* 366:14–23

- Mikhail S, Guillermier C, Franchi IA, Beard AD, Verchovsky AB, Wood I, Jones AP, Milledge HJ (2014b) Empirical evidence for the fractionation of carbon isotopes between diamond and iron carbide from the Earth's mantle. *Geochem Geophys Geosyst* 15:855–866
- Mikhail S, Howell D, McCubbin FM (2014c) Evidence for multiple diamondite forming events in the mantle. *Am Mineral* 99:1537–1543
- Mikhail S, Crosby JC, Stuart FM, Di Nicola L, Abernethy FAJ (2019a) A secretive mechanical exchange between mantle and crustal volatiles revealed by helium isotopes in  $^{13}\text{C}$ -depleted diamonds. *Geochem Perspect Lett* 11:39–43
- Mikhail S, McCubbin FE, Jenner FE, Shirey SB, Rumble D, Bowden R (2019b) Diamondites: evidence for a distinct tectonothermal diamond forming event beneath the Kaapvaal craton. *Contrib Mineral Petrol* 174:71–86
- Mikhail S, Rinaldi M, Mare ER, Sverjensky DA (2021) A genetic metasomatic link between eclogitic and peridotitic diamond inclusions. *Geochem Perspect Lett* 17:33–38
- Miller CE, Kopylova M, Smith E (2014) Mineral inclusions in fibrous diamonds: constraints on cratonic mantle refertilization and diamond formation. *Mineral Petrol* 108:317–331
- Navon O, Hutcheon ID, Rossman GR, Wasserburg GJ (1988) Mantle-derived fluids in diamond inclusions. *Nature* 335:784–789
- Orlov JL (1977) *The Mineralogy of Diamond*. Wiley, New York
- Palot M, Cartigny P, Viljoen F (2009) Diamond origin and genesis: A C and N stable isotope study on diamonds from a single eclogitic xenolith (Kaalvallei, South Africa). *Lithos* 112:758–766
- Palot M, Cartigny P, Harris JW, Kaminsky FV, Stachel T (2012) Evidence for deep mantle convection and primordial heterogeneity from nitrogen and carbon stable isotopes in diamond. *Earth Planet Sci Lett* 357:179–193
- Palot M, Pearson DG, Stachel T, Harris JW, Bulanova GP, Chinn I (2013) Multiple growth episodes or prolonged formation of diamonds? Inferences from infrared absorption data. *In: Proceedings 10<sup>th</sup> International Kimberlite Conference*. Vol 1. D Pearson DG, Grütter HS, Harris JW, Kjarsgaard BJ, O'Brien H, Chalpathi Rao NV, Sparks S (eds) Springer, p 281–296
- Petts DC, Chacko T, Stachel T, Stern RA, Heaman LM (2015) A nitrogen isotope fractionation factor between diamond and its parental fluid derived from detailed SIMS analysis of a gem diamond and theoretical calculations. *Chem Geol* 410:188–200
- Petts DC, Stachel T, Stern RA, Hunt L, Fomradas G (2016) Multiple carbon and nitrogen sources associated with the parental mantle fluids of fibrous diamonds from Diavik, Canada, revealed by SIMS microanalysis. *Contrib Mineral Petrol* 171:17–32
- Polyakov VB, Kharlashina NN (1995) The use of heat capacity data to calculate carbon isotope fractionation between graphite, diamond, and carbon dioxide: a new approach. *Geochim Cosmochim Acta* 59:2561–2572
- Porcelli D, Elliott, T (2008) The evolution of He isotopes in the convecting mantle and the preservation of high  $^3\text{He}/^4\text{He}$  ratios. *Earth Planet Sci Lett* 269:175–185.
- Rehfeldt T, Foley SF, Jacob DE, Carlson RW, Lowry D (2008) Contrasting types of metasomatism in dunite, wehrlite and websterite xenoliths from Kimberley, South Africa. *Geochim Cosmochim Acta* 72:5722–5756
- Reutsky VN, Harte B, Borzdov YN, Palyanov YN (2008) Monitoring diamond crystal growth, a combined experimental and SIMS study. *Eur J Mineral* 20:365–374
- Reutsky VN, Borzdov YN, Palyanov YN, Sokol A, Izokh O (2015) Carbon isotope fractionation during experimental crystallisation of diamond from carbonate fluid at mantle conditions. *Contrib Mineral Petrol* 170:41–50
- Richet P, Bottinga Y, Javoy M (1977) A review of hydrogen, carbon, nitrogen, oxygen, sulphur, and chlorine stable isotope enrichment among gaseous molecules. *Annu Rev Earth Planet Sci* 5:65–110
- Rohrbach A, Schmidt MW (2011) Redox freezing and melting in the Earth's deep mantle resulting from carbon-iron redox coupling. *Nature* 472:209–212
- Rubanova EV, Piazzolo S, Griffin WL, O'Reilly SY (2012) Deformation microstructures reveal a complex mantle history for polycrystalline diamond. *Geochem Geophys Geosyst* 13:Q10010
- Schollenbruch K, Woodland AB, Frost DJ, Wang Y, Sanehira T, Langenhorst F (2011) In situ determination of the spinel–post-spinel transition in  $\text{Fe}_3\text{O}_4$  at high pressure and temperature by synchrotron X ray diffraction. *Am Mineral* 96:820–827
- Shelkov DA (1997) N and C isotopic composition of different varieties of terrestrial diamond and carbonado. PhD dissertation, The Open University, Milton Keynes, UK
- Shelkov DA, Verchovsky AB, Milledge HJ, Pillinger CT (1997) Carbonado: a comparison between Brazilian and Ubangui sources with other forms of microcrystalline diamond based on carbon and nitrogen isotopes. *Russ Geol Geophys* 38:332–340
- Smelova GB (1994) Origin of Diamond Aggregates from the Kimberlite Pipes of Yakutia (Yakutsk), Novosibirsk
- Smit KV, Shirey SB, Stern RA, Steele A, Wang WY (2016) Diamond growth from C–H–N–O recycled fluids in the lithosphere: Evidence from  $\text{CH}_4$  micro-inclusions and  $\delta^{13}\text{C}$ – $\delta^{15}\text{N}$ –N content in Marange mixed-habit diamonds. *Lithos* 265:68–81
- Smith CB, Walter MJ, Bulanova GP, Mikhail S, Burnham AD, Gobbo L, Kohn SC (2016) Diamonds from Dachine, French Guiana: a unique record of Early Proterozoic subduction. *Lithos* 265:82–95
- Sobolev NV (1977) Deep-seated inclusions in kimberlites and the problem of the composition of the upper mantle. AGU, New York

- Sobolev NV, Lavrentev YG, Pokhilenko NP, Usova LV (1973) Chrome-rich garnets from the kimberlites of Yakutia and their parageneses. *Contrib Mineral Petrol* 40:39–52
- Sobolev NV, Yefimova ES, Pospelova LN (1989) Native iron in Yakutian diamonds and its paragenesis. *Soviet Geol Geophys* 22:18–21
- Sobolev NV, Shatsky VS, Zedgenizov DA, Ragozin AL, Reutsky VN (2016) Polycrystalline diamond aggregates from the Mir kimberlite pipe, Yakutia: Evidence for mantle metasomatism. *Lithos* 265:257–266
- Stachel T, Aulbach S, Brey GP, Harris JW, Leost I, Tappert R, Viljoen KS (2004) The trace element composition of silicate inclusions in diamonds: a review. *Lithos* 77:1–19
- Stachel T, Cartigny P, Chacko T, Pearson DG (2022) Carbon and nitrogen in mantle-derived diamonds. *Rev Mineral Geochem* 88:809–876
- Stachel T, Harris JW (2008) The origin of cratonic diamonds—constraints from mineral inclusions. *Ore Geol Rev* 34: 5–32
- Sun S-S, McDonough W F (1989) Chemical and isotopic systematics of oceanic basalts: implications for mantle composition and processes. *In: Magmatism in the Ocean Basins, Vol 42*, Saunders AD, Norry MJ (eds.) *Geol Soc Spec Publ*, p 313–345
- Sunagawa I (2005) *Crystals. Growth, Morphology and Perfection*. Cambridge University Press, Cambridge, New York
- Tappert R, Foden J, Stachel T, Muehlenbachs K, Tappert M, Wills K (2009) The diamonds of South Australia. *Lithos* 112:806–821
- Thomassot E, Cartigny P, Harris JW, Lorand JP, Rollion-Bard C, Chaussidon M (2009) Metasomatic diamond growth: A multi-isotope study ( $^{13}\text{C}$ ,  $^{15}\text{N}$ ,  $^{33}\text{S}$ ,  $^{34}\text{S}$ ) of sulphide inclusions and their host diamonds from Jwaneng (Botswana). *Earth Planet Sci Lett* 282:79–90
- Thomazo C, Pinti DL, Busigny V, Ader M, Hashizume K, Philippot P (2009) Biological activity and the Earth's surface evolution: Insights from carbon, sulfur, nitrogen and iron stable isotopes in the rock record. *C R Palevol* 8:665–678
- Thomson AR, Kohn SC, Prabhua A, Walter MJ (2021) Evaluating the formation pressure of diamond-hosted majoritic garnets: A machine learning majorite barometer. *J Geophys Res: Solid Earth* 126:e2020JB020604
- Timmerman S, Koornneef J, Chinn I, Davies GR (2017) Dated eclogitic diamond growth zones reveal variable recycling of crustal carbon through time. *Earth Planet Sci Lett* 463:178–188
- Timmerman S, Honda M, Phillips D, Jaques AL, Harris JW (2018) Noble gas geochemistry of fluid inclusions in South African diamonds: implications for the origin of diamond-forming fluids. *Mineral Petrol* 112:181–195
- Timmerman S, Krebs MY, Pearson DG, Honda M (2019a) Diamond-forming media through time—Trace element and noble gas systematics of diamonds formed over 3 billion years of Earth's history. *Geochim Cosmochim Acta* 257:266–283
- Timmerman S, Krebs, MY, Burnham AD, Amelin, Y, Woodland S, Pearson DG, Jaques AL, Le Sosq C, Bennet VC, Bulanova GP, Smith CB, Harris JW, Tohver E (2019b) Primordial and recycled helium isotope signatures in the mantle transition zone. *Science* 365:692–694
- Trueb LF, De Wys EC (1969) Carbonado: Natural polycrystalline diamond. *Science* 165:799–802
- Uenver-Thiele L, Woodland AB, Boffa Ballaran T, Miyajima N, Frost DJ (2017) Phase relations of Fe-Mg spinels including new high-pressure post-spinel phases and implications for natural samples. *Am Mineral* 102:2054–2064
- Viljoen KS, Phillips D, Harris JW, Robinson D (1999) Mineral inclusions in diamonds from the Venetia kimberlites, Northern Province, South Africa. *7<sup>th</sup> International Kimberlite Conferences, Extended Abstracts*, p 943–945
- Weiss Y, Kessel R, Griffin WL, Kiflawi I, Klein-BenDavid O, Bell DR, Harris JW, Navon O (2009) A new model for the evolution of diamond-forming fluids; evidence from microinclusion-bearing diamonds from Kankan, Guinea. *Lithos* 112:660–674
- Weiss Y, Griffin WL, Bell DR, Navon O (2011) High-Mg carbonatitic melts in diamonds, kimberlites and the sub-continental lithosphere. *Earth Planet Sci Lett* 309:337–347
- Weiss Y, Caza J, Navon O (2022) Fluid inclusions in fibrous diamonds. *Rev Mineral Geochem* 88:475–532
- Wiggers de Vries DF, Bulanova GP, De Corte K, Pearson DG, Craven JA, Davies GR (2013) Micron-scale coupled carbon isotope and nitrogen abundance variations in diamonds: evidence for episodic diamond formation beneath the Siberian Craton. *Geochim Cosmochim Acta* 100:176–199
- Wijbrans CH, Rohrbach A, Klemme S (2016) An experimental investigation of the stability of majoritic garnet in the Earth's mantle and an improved majorite geobarometer. *Contrib Mineral Petrol* 171:50
- Wirth R (2009) Focused Ion Beam (FIB) combined with SEM and TEM: advanced analytical tools for studies of chemical composition, microstructure and crystal structure in geomaterials on a nanometre scale. *Chem Geol* 261:217–229
- Woodland AB, Frost DJ, Trots DM, Klimm K, Mezouar M (2012) In situ observation of the breakdown of magnetite ( $\text{Fe}_3\text{O}_4$ ) to  $\text{Fe}_2\text{O}_3$  and hematite at high pressures and temperatures. *Am Mineral* 97:1808–1811
- Woods GS (1986) Platelets and the infrared-absorption of type-Ia diamonds. *Proc R Soc Lond Ser A Math Phys Eng Sci* 407:219–23

